Alternative isoforms of KDM2A and KDM2B lysine demethylases negatively regulate canonical Wnt signaling

Dijana Lađinović[¶], Daniel Pinkas[¶], Otakar Raška, František Liška, Ivan Raška,

Tomáš Vacík*

Institute of Biology and Medical Genetics, First Faculty of Medicine, Charles University and General

University Hospital in Prague, Albertov 4, Praha 2, Czech Republic

*Corresponding author: tomas.vacik@lf1.cuni.cz

[¶]These authors contributed equally to this work.

13   **Abstract**

14   A precisely balanced activity of canonical Wnt signaling is essential for a number of biological

15   processes and its perturbation leads to developmental defects or diseases. Here, we demonstrate

16   that alternative isoforms of the KDM2A and KDM2B lysine demethylases have the ability to

17   negatively regulate canonical Wnt signaling. These KDM2A and KDM2B isoforms (KDM2A-SF and

18   KDM2B-SF) lack the N-terminal demethylase domain, but they are able to bind to activated

19   promoters in order to repress them. We have observed that KDM2A-SF and KDM2B-SF bind to

20   and repress the promoters of AXIN2 and CYCLIN D1, two canonical Wnt signaling target genes.

21   Moreover, KDM2A-SF and KDM2B-SF can repress a Wnt-responsive luciferase reporter. The

22   transcriptional repression mediated by KDM2A-SF and KDM2B-SF, but also by KDM2A-LF, is

23   dependent on their DNA binding domain, while the N-terminal demethylase domain is dispensable

24   for this process. Surprisingly, KDM2B-LF is unable to repress both the endogenous promoters and

25   the luciferase reporter. Finally, we show that both KDM2A-SF and KDM2B-SF are able to interact

26   with TCF7L1, one of the transcriptional mediators of canonical Wnt signaling. KDM2A-SF and

27   KDM2B-SF are thus likely to affect the transcription of the TCF7L1 target genes also through this

28   interaction.

29   **Introduction**

30   KDM2A and KDM2B (KDM2A/B) are two closely related lysine demethylases with the ability

31   to bind to non-methylated CpG islands through their CXXC DNA binding domain. After binding to

32   non-methylated CpG islands in transcriptionally active promoters, KDM2A/B demethylate mono- and

33   di-methylated H3K36 lysines (H3K36me1/2) using their N-terminal Jumonji-C demethylase domain

34   (1, 2). KDM2B is able to demethylate also H3K4me3 (3). By demethylating H3K36me1/2 and

35   H3K4me3 in transcriptionally active promoters (4-6), KDM2A/B function as transcriptional repressors

36   of the promoters that contain CpG islands (1, 7-10). Although KDM2A and KDM2B have very similar

37   structure, they have been shown to interact with different protein partners to repress different target

38   regions. For example, KDM2A interacts with HP1a to repress the pericentromeric heterochromatin

39   (11-13), whereas KDM2B forms complex with the PRC1 complex to silence developmentally

40   important genes in embryonic stem cells (10).

41   Interestingly, KDM2A has been shown to interact with and to demethylate also non-histone

42   proteins such as the p65 subunit of NF-kappaB or beta-catenin (14, 15). Beta-catenin is the key

43   mediator of canonical Wnt signaling, which plays an essential role in a number of processes ranging

44   from embryogenesis to aging, and whose malfunction frequently leads to various developmental

45   defects and diseases including cancer (16-21). After activation of the pathway by Wnt ligands, beta-

46   catenin enters the nucleus where it teams up with TCF/LEF transcription factors (TCF7L1, TCF7L2,

47   TCF7, and LEF1) to activate transcription of their target genes. In the absence of Wnt ligands beta-

48   catenin is phosphorylated at its N-terminal serines and threonines by the GSK-3/CKI kinases, which

49   subsequently leads to its ubiquitination and finally to its proteasome mediated degradation. In the

50   absence of beta-catenin in the nucleus, TCF/LEF proteins team up with co-repressors to act as

51   transcriptional repressors of their target genes (16, 19, 22, 23). Interestingly, it has been

52   demonstrated that KDM2A can displace the nuclear beta-catenin from the complex with TCF7L1,

53   which results in transcriptional repression of the TCF7L1 target genes (14).

54   The same loci that encode the full-length KDM2A/B proteins (KDM2A/B-LF) also encode

55   shorter KDM2A proteins that lack the N-terminal demethylase domain (1). However, these

56   alternative short isoforms (KDM2A/B-SF) share all the other functional domains with KDM2A/B-LF.

57   Therefore, KDM2A/B-SF are not able to demethylate the KDM2A/B target lysines, but they still have

58   the ability to bind to the same DNA regions as KDM2A/B-LF and to interact with the same proteins

59   as KDM2A/B-LF. KDM2A/B-SF are thus likely to compete with KDM2A/B-LF or to complement their

60   function (1). Despite the fact that a KDM2A-SF specific knockout mutant has not been described yet

61   and it cannot be compared to the embryonically lethal KDM2A-LF knockout phenotype (24), we

62   previously showed that the distinct KDM2A positive nuclear structures on pericentromeric

63   heterochromatin are formed by KDM2A-SF and not by KDM2A-LF (12). Similarly, the fact that the

64   KDM2B-SF specific knockout phenotype is different from that of the KDM2B-LF loss-of-function

65   mutants also implies different functions for the short and long isoforms (25-27).

66   Here we asked whether KDM2A/B-SF also affect canonical Wnt signaling despite lacking the

67   demethylase domain. We demonstrate that both KDM2A-SF and KDM2B-SF have the ability to

68   negatively regulate this signaling pathway by binding to and repressing the CpG island containing

69   promoters of the pathway components AXIN2 and CYCLIN D1. Moreover, we found that KDM2A-

70   SF and KDM2B-SF can interact with TCF7L1, one of the TCF/LEF transcriptional mediators of the

71   pathway, which further broadens the negative effects that KDM2A/B-SF have on the TCF/LEF target

72   genes.

73   **Material and Methods**

74   **Cells**

75   HEK293T cells were grown in 5% CO_2 at 37°C and in the high glucose DMEM medium supplemented

76   with 10% fetal bovine serum and the PenStrep antibiotics (all ThermoFisher Scientific). To stabilize

77   beta-catenin and to induce canonical Wnt signaling the cells were treated with 1 μM BIO (6-

78   Bromoindirubin-3′-oxime, SIGMA B1686) for 24 hours before harvesting.

79   **Plasmids and transfection**

80   The coding regions of the corresponding genes were amplified by RT-PCR using the primers listed

81   in supplementary table S1. The RT-PCR products were cloned in the pCS2 expression plasmids and

82   the constructs were verified by sequencing. The mutant constructs were prepared by PCR

83   mutagenesis using the Phusion polymerase (ThermoFisher Scientific). The TOP5 and FOP5

84   luciferase constructs were described previously (28). The *AXIN2* promoter luciferase constructs were

85   prepared by PCR using the primers listed in supplementary table S1. The PCR products were cloned

86   into the luciferase pNL1.1 vector (Promega) and verified by sequencing. The plasmids were

87   transfected into cells using Fugene6 (Promega) or Turbofect (ThermoFisher Scientific).

88   **RNA and Q-RT-PCR**

89   Total RNA was prepared with TRIzol (ThermoFisher Scientific) according to the manufacturer's

90   instructions and reverse transcribed with the LunaScript RT SuperMix kit (NEB). cDNA was analyzed

91   by quantitative PCR using the CFX96 Touch Real-Time PCR Detection System (BIO-RAD),

92   PowerUP SYBR Green mix (ThermoFisher Scientific), and the primers listed in supplementary table

93   S1. The results were analyzed using the CFX Maestro software (BIO-RAD) and are presented as

94   means ±SD of at least three independent experiments. The significance was determined using the

95   student t-test.

96   **Luciferase reporter assay**

97   Cells were co-transfected with the pNL1.1 nano luciferase reporter constructs, expression constructs

98   and control firefly construct using Fugene6 (Promega). The reporter assays were performed using

99   the NanoGlo Dual luciferase system (Promega) and the Infinite 200 luminometer (Tecan). To induce

100   the transcription of the canonical Wnt signaling target genes, the cells were either treated with the

101   pathway agonist BIO (1 μM, 24 hrs, SIGMA B1686) or transfected with the pCS2-beta-catenin

102   expression constructs. The results are presented as means ±SD of at least three independent

103   experiments.

104   **Proteins and western blot**

105   Whole cell extracts were prepared by rotating the cell pellets for 2 hrs at + 4°C in five volumes of the

106   high salt lysis buffer (50 mM Tris, 300 mM NaCl, 10% glycerol, 0.5% NP-40, 1x cOmplete ULTRA

107   protease inhibitors (Roche)). Proteins were resolved on 10% SDS-PAGE gels, transferred to the

108   Immobilon-P/E PVDF membrane (Merck Millipore), and immunodetected using the SuperSignal

109   West Pico PLUS Chemiluminescent Substrate (ThermoFisher Scientific) and the following

110   antibodies: anti-FLAG M2 (Sigma, F1804), anti-DYKDDDDK Tag (Cell Signaling, 14793), anti-Myc

111   Tag (Millipore, 05-724), anti-mouse-HRP (GE healthcare, NA931-1ML), anti-rabbit-HRP (GE

112   healthcare, NA934-1ML).

113   **Co-immunoprecipitation**

114   HEK293T cells were transfected with the corresponding FLAG tag expression constructs using

115   Turbofect (ThermoFisher Scientific). The whole cell extracts were prepared as described in 2.6. and

116   diluted to 150 mM NaCl and 0.1% NP-40. 500 μg of the whole cell extract was rotated overnight at +

117   4°C with 2.5 μg of the anti-FLAG antibody (Sigma F1804) and the protein-immunocomplexes were

118   separated with the Dynabeads Protein G magnetic beads (ThermoFisher Scientific). Proteins were

119   eluted by boiling the beads in the LDS sample buffer (ThermoFisher Scientific) and analyzed by

120   western blot.

121   **Chromatin immunoprecipitation**

122   HEK293T cells were transfected with the pCS2-FLAG empty and protein coding constructs using

123   Turbofect (ThermoFisher Scientific). After 48 hrs the cells were crosslinked with 1% formaldehyde

124   (ThermoFisher Scientific) for 15 minutes at room temperature. The crosslinking reaction was

125   stopped by 0.125M glycine and the samples were processed using the MAGnify Chromatin

126   Immunoprecipitation System (ThermoFisher Scientific), Bioruptor (Diagenode), the anti-FLAG

127   antibody (Sigma, F1804), anti-H3K4me3 (Cell Signaling, 9751), and the control IgG (Sigma, 12-

128   371). The immunoprecipiated DNA was analyzed using the CFX96 Touch Real-Time PCR Detection

129   System (BIO-RAD), Luna Universal qPCR Master Mix (NEB), and the primers listed in

130   supplementary table S1. The HEK293T cells transfected on the same day with the same constructs

131   were used to verify the expression of the FLAG-tagged proteins by western blot.

132   **Results**

133   **KDM2A-SF and KDM2B-SF repress a Wnt-Responsive Luciferase Reporter**

134   Since KDM2A-LF has been previously shown to strongly repress the Wnt-responsive luciferase

135   Topflash reporter activated by elevated levels of beta-catenin (14), we set out to test whether the

6

136 KDM2A-SF and KDM2B-SF isoforms are also able to repress this reporter despite lacking the

137 demethylase domain. We used the TCF/LEF luciferase reporter TOP5, in which the luciferase gene

138 is under the control of five TCF/LEF consensus binding sites and which thus reflects the activity of

139 canonical Wnt signaling (Fig.1A)(28). We activated the canonical Wnt pathway in HEK293T cells

140 with the pathway agonist BIO (6-Bromoindirubin-3′-oxime). BIO blocks the function of glycogen

141 synthase kinase-3 (GSK3), whose role is to phosphorylate beta-catenin in the absence of a Wnt

142 ligand and by doing so to prevent it from entering the nucleus (16, 18). Blocking the function of GSK3

143 results in accumulation of non-phosphorylated beta-catenin, its nuclear deposition and consequently

144 in activation of TCF/LEF target genes including the above-mentioned TCF/LEF responsive TOP5

145 luciferase reporter (14, 29-34). Our luciferase reporter experiments confirmed that elevated levels

146 of KDM2A-LF lead to a repression of the activated reporter, but they further showed that both

147 KDM2A-SF or KDM2B-SF are also able to strongly repress this Wnt-responsive reporter despite

148 lacking the N-terminal demethylase domain (Figs.1B and 1C). Interestingly, the full-length KDM2B-

149 LF protein was not able to repress the activated TOP5 reporter (Fig.1C).

150
151 **Fig.1. KDM2A-SF and KDM2B-SF repress the canonical Wnt signaling luciferase reporter. A.**

152 The wild type TCF/LEF reporter (TOP5) contains five TCF/LEF consensus binding sites (CTTTGAT)

153 that drive the expression of the luciferase gene. The FOP5 construct contains five mutant TCF/LEF

154 binding sites (CTTTGCC) instead and serves as the background activity control. **B.** Both KDM2A-

155 LF and KDM2A-SF strongly repressed the TOP5 reporter activated with BIO. The reporter activity is

156 expressed as the fold change ratio between the normalized luciferase signal of TOP5 and FOP5. **C.**

157 KDM2B-SF, but not KDM2B-LF, also strongly repressed the activated reporter. **D.** Repression of the

158 TOP5 reporter by KDM2A is not dependent on the activity of its JmjC demethylase domain, but

159 predominantly on the CXXC DNA binding domain. **E.** KDM2B was not able to repress the activated

160 TOP5 reporter, whereas KDM2B-SF strongly repressed it in a DNA binding domain dependent

161 manner. (*$p < 0.05$; **$p < 0.01$).

162

163   We observed similar repression patterns when the TOP5 reporter was stimulated by the

164   overexpression of beta-catenin (data not shown). These results imply that the N-terminal

165   demethylase domain of KDM2A is not behind the transcriptional repressive effect that KDM2A has

166   on the TOP5 reporter. To analyze that the activity of the JmjC demethylase domain is not required

167   for the repressive effect, we performed the same reporter experiment with the KDM2A protein

168   bearing the mutations previously shown to disrupt the function of the KDM2A demethylase domain,

169   H212A and D214A (35). This experiment confirmed that the activity of the JmjC demethylase domain

170   is dispensable for the KDM2A-mediated repression of the TOP5 reporter (Fig.1D). Surprisingly, the

171   K601A mutation that disrupts the CXXC DNA binding domain of KDM2A not only reverted the

172   repressive effect of both KDM2A-LF and KDM2A-SF, but it had a positive regulatory effect on the

173   TOP5 reporter (Fig.1D, mutJmjC)(35). Similarly, disruption of the PHD domain by the C620A/C623A

174   mutations abolished the repressive abilities of both KDM2A-LF and KDM2A-SF (Fig.1D,

175   mutPHD)(11). Unlike KDM2B, KDM2A contains a short aminoacid motif that is important for the

176   interaction with the heterochromatin protein HP1 (11). Disruption of this HP1 motif by the V801A

177   and V803A substitutions reverted the repressive effect of KDM2A-LF, but not that of KDM2A-SF

178   (Fig.1D, mutHP1a). As already stated above, KDM2B-LF did not repress the TOP5 reporter and

179   mutating its functional domains had no significant effect in this regard (Fig.1E). On the other hand,

180   the strong repression of the TOP5 reporter by KDM2B-SF was also dependent on its DNA-binding

181   domain, whereas its PHD domain seems dispensable for this repression (Fig.1E).

182   **KDM2A-SF and KDM2B-SF repress transcription of AXIN2 and CYCLIN D1**

183   To complement our luciferase reporter data and to analyze whether KDM2A-SF and KDM2B-SF are

184   able to repress also endogenous canonical Wnt signaling target genes, we focused on AXIN2 and

185   CYCLIN D1. AXIN2 and CYCLIN D1 are two widely studied direct target genes of canonical Wnt

186   signaling and as such their promoters can be activated with BIO (36-40). We stimulated their

187   expression with BIO and analyzed their transcriptional activity by Q-RT-PCR in the presence of the

188   above described KDM2A and KDM2B protein variants. Consistently with our luciferase assays, both

189   KDM2A-LF and KDM2A-SF strongly repressed activated AXIN2 and CYCLIN D1 (Figs.2A and 2B).

190   While the transcriptional repression of AXIN2 by both KDM2A-LF and KDM2A-SF is dependent on

191   their CXXC DNA binding domain, disruption of this domain did not completely revert the repressive

192   effect on CYCLIN D1 (Figs.2A and 2B, mutCXXC). However, the KDM2A-LF mediated repression

193   of the *CYCLIN D1* gene seems to be dependent on the HP1 motif, whose disruption reverted the

194   repressive effect (Fig.2B, mutHP1a). This implies that the nature of the *CYCLIN D1* transcriptional

195   regulation by the KDM2A isoforms is different from that of AXIN2. Consistently with the results of

196   our luciferase assay, KDM2B-LF failed to repress both AXIN2 and CYCLIN D1 (Figs.2C and 2D).

197   On the other hand, KDM2B-SF efficiently repressed both AXIN2 and CYCLIN D1 in a DNA binding

198   domain dependent manner, since disruption of its CXXC domain by the C586/589/592A mutations

199   reverted the repression (Figs.2C and 2D)(41). The C661/664A mutations that disrupt the KDM2B

200   PHD domain had no significant effect and these KDM2B mutant proteins still repressed both AXIN2

201   and CYCLIN D1 (Figs.2C and 2D)(42).

202
203   **Fig.2. KDM2A-SF and KDM2B-SF repress AXIN2 and CYCLIN D1. A.** Both KDM2A-LF and

204   KDM2A-SF repressed AXIN2 in a DNA binding domain dependent manner. **B.** When activated with

205   BIO, CYCLIN D1 is also repressed by both KDM2A-LF and KDM2A-SF, but independently of the

206   DNA binding domain. **C.** Similarly to KDM2A-SF, KDM2B-SF repressed activated AXIN2, whereas

207   KDM2B-LF had no effect on its transcription. **D.** CYCLIN D1 was also repressed by KDM2B-SF, but

208   not by KDM2B-LF. The mRNA levels were determined by Q-RT-PCR and are related to GAPDH.

209   Similar patterns were obtained also with HPRT and RPL32 (*$p < 0.05$; **$p < 0.01$).

210

211   **KDM2A-SF and KDM2B-SF repress AXIN2 promoter**

212   Transcriptional repression of AXIN2 and CYCLIN D1 by KDM2A-LF, KDM2A-SF and KDM2B-SF is

213   well consistent with the fact that KDM2A/B act as CpG island binding transcriptional repressors (1).

214   Since the *AXIN2* and *CYCLIN D1* promoters contain CpG islands, the KDM2A/B-SF mediated

215   repression of these promoters is likely to be direct. To investigate whether KDM2A-SF and KDM2B-

216   SF directly repress the *AXIN2* promoter, we focused on the *AXIN2* promoter region in its first intron

217   (Fig.3A). This intronic promoter region contains a CpG island and it has been shown to act as an

218   important regulatory promoter element of AXIN2 (38). The ENCODE ChIP-seq data that are publicly

219   available via the UCSC genome browser further show that this region is bound by RNA-POL II and

220   various transcription factors in multiple cell lines, which further confirms its importance for the

221   transcriptional regulation of AXIN2 (43). Consistently with the above mentioned facts, this

222   approximately 2.5 kb *AXIN2* intron 1 region exhibited a high transcription inducing activity in a

223   luciferase assay as opposed to a shorter approximately 1 kb *AXIN2* intron 1 region that lacks the

224   CpG island (Figs.3A and 3B). Consistently with our TOP5 reporter and Q-RT-PCR results, the

225   luciferase activity driven by this *AXIN2* promoter region was repressed by KDM2A-LF, KDM2A-SF,

226   and KDM2B-SF, whereas KDM2B-LF was not able to repress this region (Fig.3B).

227

228   **Fig.3. KDM2A-SF and KDM2B-SF repress AXIN2 promoter. A.** The *AXIN2* promoter luciferase

229   reporter constructs contain either a 1kb *AXIN2* intron 1 region (pAXIN2-1kb) or a 2.5kb *AXIN2* intron

230   1 region (pAXIN2-2.5kb). **B.** KDM2A-LF, KDM2A-SF and KDM2B-SF all repressed the pAXIN2-

231   2.5kb reporter, whereas KDM2B-LF did not. The activity of the pAXIN2-2.5kb reporter is expressed

232   as the fold change ratio between the activity of pAXIN2-2.5kb and that of pAXIN2-1kb. Similar

233   pattern was observed when the results were expressed as the fold change between the activity of

234   pAXIN2-2.5kb and the empty luciferase plasmid. (*p < 0.05; **p < 0.01).

235

236   **KDM2A-SF and KDM2B-SF bind to the repressed AXIN2 and CYCLIND1 promoter regions**

10

237   Our results imply that KDM2A-SF and KDM2B-SF directly repress the transcription of AXIN2 and

238   CYCLIN D1. To test whether KDM2A/B-SF isoforms directly bind to the promoters of these genes

239   we performed a series of chromatin immunoprecipitation (ChIP) assays. The amino acid sequence

240   of the alternative KDM2A/B-SF isoforms is identical to that of the corresponding region of the

241   canonical full-length KDM2A/B-LF proteins (1). Therefore, it is not possible to prepare antibodies

242   specific for KDM2A-SF and KDM2B-SF. To discriminate between binding of the long and short

243   isoforms of KDM2A/B, we overexpressed their N-terminally FLAG-tagged versions in HEK293T cells

244   and tested the selected regions for their presence by ChIP. In our ChIP assay we focused on the

245   promoter regions that have been previously shown to be important for transcriptional regulation of

246   AXIN2 and CYCLIN D1 (38-40). Furthermore, our *in silico* analysis of the publicly available data

247   showed that these regions contain CpG islands, which makes them potential targets of the KDM2A/B

248   CpG island binding proteins, and that they are bound by multiple transcription factors in various cell

249   lines, which further confirms their role in transcriptional regulation of the associated genes (43).

250   Consistently with the results of our Q-RT-PCR and luciferase experiments, the ChIP assay showed

251   that KDM2A-LF, KDM2A-SF and KDM2B-SF bind to the promoter of AXIN2, whereas KDM2B-LF

252   does not (Figs.4A and 4B). Moreover, we tested the same *AXIN2* promoter region for the levels of

253   H3K4me3, the histone lysine methylation associated with transcriptionally active regions (4, 5). This

254   ChIP experiment revealed that the H3K4me3 levels on the *AXIN2* promoter expectedly rise after the

255   treatment with BIO, whereas they fall back in the presence of KDM2A-LF or KDM2A-SF (Fig.4C).

256   These changes in the H3K4me3 levels are consistent with the transcriptional activation of the *AXIN2*

257   promoter with BIO and with the KDM2A/B-SF mediated repression of this promoter, respectively.

258   Similarly, the *CYCLIN D1* promoter was bound by KDM2A-LF, KDM2A-SF and KDM2B-SF, but not

259   by KDM2B-LF (Figs.4D and 4E), and its H3K4me3 levels are also lower in the presence of KDM2A-

260   LF or KDM2A-SF (Fig.4F).

261

262   **Fig.4. KDM2A-SF and KDM2B-SF bind to the repressed AXIN2 and CYCLIND1 promoter**

263   **regions. A.** KDM2A-LF and KDM2A-SF both bind to the *AXIN2* promoter. **B.** Only KDM2B-SF, but

264   not KDM2B-LF, binds to the *AXIN2* promoter. **C.** The levels of H3K4me3 on the *AXIN2* promoter rose

265   after the treatment with BIO and then decreased in the presence of the KDM2A isoforms. **D.** KDM2A-

266   SF binds to the *AXIN2* promoter with a higher efficiency than KDM2A-LF. **E.** KDM2B-SF, but not

267   KDM2B-LF, binds to the *CYCLIN D1* promoter. **F.** The KDM2A isoforms negatively affected the

268   H3K4me3 levels also on the *CYCLIN D1* promoter. **G.** The negative control region did not co-

269   immunoprecipitate with the KDM2A/B isoforms. (*p < 0.05; **p < 0.01).

270

271   **KDM2A-SF and KDM2B-SF interact with TCF7L1**

272   Since KDM2A-LF has been shown to form a complex with TCF7L1 (14), we set out to investigate

273   whether KDM2A-SF and KDM2B-SF are also able to interact with this transcriptional mediator of

274   canonical Wnt signaling. Our co-immunoprecipitation (Co-IP) assays confirmed that tagged KDM2A-

275   LF and TCF7L1 overexpressed in HEK293T interact (Fig.5). In addition, our Co-IP experiments

276   revealed that both short isoforms, KDM2A-SF and KDM2B-SF, and the canonical full-length KDM2B-

277   LF isoform are also able to form complex with TCF7L1 (Fig.5). These results imply that the N-terminal

278   demethylase domain of the KDM2A/B demethylases is not necessary for the interaction with TCF7L1.

279   Furthermore, these interactions help explain why KDM2A-SF and KDM2B-SF can repress the

280   TCF/LEF-responsive TOP5 luciferase reporter (Fig.1), although the promoter of this reporter does

281   not contain any CpG island.

282

283   **Fig.5. Both the canonical and the demethylase domain deficient isoforms of KDM2A and**

284   **KDM2B interact with TCF7L1.** The myc-tagged TCF7L1 was overexpressed in HEK293T cells

285   together with the FLAG-tagged KDM2A/B isoforms and the proteins immunoprecipitated with anti-

286   FLAG antibody were analyzed by western blot. All the four FLAG-tagged KDM2A/B isoforms co-

287   immunoprecipitated with TCF7L1. The input corresponds to 5% of the whole cell extract that was

288   used for each immunoprecipitation reaction.

289

290   **Discussion**

291   In this study, we demonstrate that KDM2A-SF and KDM2B-SF, the two alternative isoforms of the

292   lysine demethylases KDM2A and KDM2B that lack the demethylase domain, are able to negatively

293   affect canonical Wnt signaling at the transcriptional level. We demonstrate that KDM2A-SF and

294   KDM2B-SF bind to and repress the promoters of the canonical Wnt signaling target genes AXIN2

295   and CYCLIN D1. The *AXIN2* and *CYCLIN D1* promoter regions we focused on here have been

296   previously studied and shown to be important for transcriptional regulation of the two genes (38-40).

297   The regulatory function of these regions is further supported by the publicly available ENCODE

298   ChIP-seq data, which indicate that these regions are bound by RNA-POL II and multiple transcription

299   factors in various cell lines (43). Moreover, we found that these regulatory regions contain CpG

300   islands, which makes them potential targets of KDM2A and KDM2B, and also of KDM2A-SF and

301   KDM2B-SF, since all these protein isoforms are CpG island binding proteins. The binding of KDM2A

302   and KDM2B to these CpG islands in mouse embryonic stem cells have already been experimentally

303   verified by ChIP-seq (10, 35). However, pan-antibodies that recognize both the canonical long

304   (KDM2A/B-LF) and the short (KDM2A/B-SF) isoforms were used in these studies and they are thus

305   not informative as to what isoforms are bound to these promoter regions.

306   Since KDM2A-SF and KDM2B-SF have the identical aminoacid sequence as the

307   corresponding regions of the long KDM2A/B-LF isoforms (1), it is not possible to prepare antibodies

308   specific just for KDM2A/B-SF. To circumvent this obstacle, we used FLAG-tagged versions of

309   KDM2A/B-SF and KDM2A/B-LF proteins to immunoprecipitate the chromatin regions bound by them

310   by ChIP. Our ChIP assay demonstrated that both isoforms of KDM2A, KDM2A-LF and KDM2A-SF,

311   bind to the CpG island containing promoter region of both AXIN2 and CYCLIN D1 (Figs.4A and 4D),

13

312   which is consistent with the ability of these protein isoforms to repress the transcription driven by

313   these promoters (Fig.2)., and to repress the *AXIN2* promoter luciferase construct (Fig3). Using ChIP,

314   we also analyzed the selected regions for the levels of H3K4me3, a mark of transcriptionally active

315   promoter regions (4, 5). Consistently with the transcriptional activation of AXIN2 and CYCLIN D1

316   upon stimulation of canonical Wnt signaling (Fig.2), the H3K4me3 levels in the tested promoter

317   regions rose after the treatment with BIO (Fig.4). The ChIP assay showed that the presence of either

318   KDM2A-LF or KDM2A-SF results in statistically lower H3K4me3 levels, which corresponds to the

319   transcriptionally repressive effect of these proteins on the tested promoters (Fig.4). We detected

320   similar results also for KDM2B-SF, whose binding to the two tested promoter regions leads to lower

321   H3K4me3 levels (data not shown) and to transcriptional repression of the corresponding genes

322   (Fig.2). Surprisingly, KDM2B-LF was unable to bind to the tested promoter regions, which is

323   consistent with the fact that this canonical long KDM2B protein isoform failed to repress the

324   transcription of AXIN2 and CYCLIN D1 (Fig.2). The direct repressive effect of KDM2A-LF, KDM2A-

325   SF, and KDM2B-SF on the *AXIN2* promoter is further supported by our luciferase assays, which

326   show that the *AXIN2* promoter region is repressed by these protein isoforms, whereas KDM2B-LF

327   again failed to show any transcriptionally repressive properties (Fig.3).

328   These results are further consistent with the fact that KDM2A-LF, KDM2A-SF, and KDM2B-

329   SF, but not KDM2B-LF, are able to repress the stimulated TOP5 luciferase reporter (Fig.1).

330   However, the TOP5 reporter does not contain any CpG island and so the repressive effect is either

331   not dependent on the CpG island binding domain or it is mediated by some auxiliary protein. Our

332   luciferase data demonstrate that KDM2A-SF and KDM2B-SF need their DNA binding domain to

333   repress the reporter and the KDM2A PHD domain is also involved to some extent (Fig.1). Based on

334   the previously described interaction of KDM2A-LF with TCF7L1 (14), and on the fact that the

335   luciferase gene is driven from the TOP5 plasmid by five TCF/LEF binding sites, we hypothesized

336   that the repression of the TOP5 reporter by KDM2A/B-SF might be mediated by TCF7L1. Therefore,

337   we tested whether KDM2A/B-SF are also able to interact with TCF7L1 by Co-IP. Our Co-IP results

338   indeed show that all the four KDM2A/B isoforms can interact with TCF7L1 (Fig.5). KDM2A/B-SF are

339   thus likely to repress the TCF/LEF reporter, but also endogenous TCF/LEF target promoters, by

340   interacting with TCF7L1. Our Co-IP results further indicate that the N-terminal region of KDM2A/B

341   is not necessary for the interaction with TCF7L1.

342   In this study, we present a mechanism that regulates the canonical Wnt signaling activity at

343   the transcriptional level through KDM2A-SF and KDM2B-SF. KDM2A-SF and KDM2B-SF have the

344   ability to affect canonical Wnt signaling by both binding to the promoters of canonical Wnt signaling

345   target genes such as AXIN2 or CYCLIN D1, and by interacting with TCF7L1.

References

347 1. Vacik T, Ladinovic D, Raska I. KDM2A/B lysine demethylases and their alternative isoforms in
348   development and disease. Nucleus. 2018;9(1):431-41.

349 2. Tsukada Y, Fang J, Erdjument-Bromage H, Warren ME, Borchers CH, Tempst P, et al. Histone
350   demethylation by a family of JmjC domain-containing proteins. Nature. 2006;439(7078):811-6.

351 3. Janzer A, Stamm K, Becker A, Zimmer A, Buettner R, Kirfel J. The H3K4me3 histone
352   demethylase Fbxl10 is a regulator of chemokine expression, cellular morphology, and the
353   metabolome of fibroblasts. J Biol Chem. 2012;287(37):30984-92.

354 4. Gates LA, Foulds CE, O'Malley BW. Histone Marks in the 'Driver's Seat': Functional Roles in
355   Steering the Transcription Cycle. Trends Biochem Sci. 2017;42(12):977-89.

356 5. Black JC, Van Rechem C, Whetstine JR. Histone lysine methylation dynamics: establishment,
357   regulation, and biological impact. Mol Cell. 2012;48(4):491-507.

358 6. Zaghi M, Broccoli V, Sessa A. H3K36 Methylation in Neural Development and Associated
359   Diseases. Front Genet. 2019;10:1291.

360 7. Dhar SS, Alam H, Li N, Wagner KW, Chung J, Ahn YW, et al. Transcriptional repression of
361   histone deacetylase 3 by the histone demethylase KDM2A is coupled to tumorigenicity of lung
362   cancer cells. J Biol Chem. 2014;289(11):7483-96.

363 8. Wagner KW, Alam H, Dhar SS, Giri U, Li N, Wei Y, et al. KDM2A promotes lung tumorigenesis
364   by epigenetically enhancing ERK1/2 signaling. J Clin Invest. 2013;123(12):5231-46.

365 9. He J, Kallin EM, Tsukada Y, Zhang Y. The H3K36 demethylase Jhdm1b/Kdm2b regulates cell
366   proliferation and senescence through p15(Ink4b). Nat Struct Mol Biol. 2008;15(11):1169-75.

367 10. Farcas AM, Blackledge NP, Sudbery I, Long HK, McGouran JF, Rose NR, et al. KDM2B links
368   the Polycomb Repressive Complex 1 (PRC1) to recognition of CpG islands. eLife.
369   2012;1:e00205.

370 11. Borgel J, Tyl M, Schiller K, Pusztai Z, Dooley CM, Deng W, et al. KDM2A integrates DNA and
371   histone modification signals through a CXXC/PHD module and direct interaction with HP1.
372   Nucleic Acids Res. 2017;45(3):1114-29.

373 12. Ladinovic D, Novotna J, Jaksova S, Raska I, Vacik T. A demethylation deficient isoform of the
374   lysine demethylase KDM2A interacts with pericentromeric heterochromatin in an HP1a-
375   dependent manner. Nucleus. 2017;8(5):563-72.

376 13. Frescas D, Guardavaccaro D, Kuchay SM, Kato H, Poleshko A, Basrur V, et al. KDM2A
377   represses transcription of centromeric satellite repeats and maintains the heterochromatic
378   state. Cell Cycle. 2008;7(22):3539-47.

379 14. Lu L, Gao Y, Zhang Z, Cao Q, Zhang X, Zou J, et al. Kdm2a/b Lysine Demethylases Regulate
380   Canonical Wnt Signaling by Modulating the Stability of Nuclear beta-Catenin. Dev Cell.
381   2015;33(6):660-74.

382 15. Lu T, Jackson MW, Wang B, Yang M, Chance MR, Miyagi M, et al. Regulation of NF-kappaB
383   by NSD1/FBXL11-dependent reversible lysine methylation of p65. Proc Natl Acad Sci U S A.
384   2010;107(1):46-51.

385 16. Nusse R, Clevers H. Wnt/beta-Catenin Signaling, Disease, and Emerging Therapeutic
386   Modalities. Cell. 2017;169(6):985-99.

387 17. Anastas JN, Moon RT. WNT signalling pathways as therapeutic targets in cancer. Nat Rev
388   Cancer. 2013;13(1):11-26.

389 18. Clevers H, Nusse R. Wnt/beta-catenin signaling and disease. Cell. 2012;149(6):1192-205.

390 19. MacDonald BT, Tamai K, He X. Wnt/beta-catenin signaling: components, mechanisms, and
391   diseases. Dev Cell. 2009;17(1):9-26.

392 20. Sokol SY. Maintaining embryonic stem cell pluripotency with Wnt signaling. Development.
393   2011;138(20):4341-50.

394 21. Cadigan KM, Peifer M. Wnt signaling from development to disease: insights from model
395   systems. Cold Spring Harbor perspectives in biology. 2009;1(2):a002881.

396 22. Stamos JL, Weis WI. The beta-catenin destruction complex. Cold Spring Harbor
397   perspectives in biology. 2013;5(1):a007898.

398 23. Fagotto F. Looking beyond the Wnt pathway for the deep nature of beta-catenin. EMBO
399   Rep. 2013;14(5):422-33.

400 24. Kawakami E, Tokunaga A, Ozawa M, Sakamoto R, Yoshida N. The histone demethylase
401   Fbxl11/Kdm2a plays an essential role in embryonic development by repressing cell-cycle
402   regulators. Mech Dev. 2015;135:31-42.

403   25.   Boulard M, Edwards JR, Bestor TH. Abnormal X chromosome inactivation and sex-specific
404   gene dysregulation after ablation of FBXL10. Epigenetics & chromatin. 2016;9(22):22.

405   26.   Andricovich J, Kai Y, Peng W, Foudi A, Tzatsos A. Histone demethylase KDM2B regulates
406   lineage commitment in normal and malignant hematopoiesis. J Clin Invest.
407   2016;126(3):905-20.

408   27.   Fukuda T, Tokunaga A, Sakamoto R, Yoshida N. Fbxl10/Kdm2b deficiency accelerates
409   neural progenitor cell death and leads to exencephaly. Mol Cell Neurosci. 2011;46(3):614-
410   24.

411   28.   Vacik T, Stubbs JL, Lemke G. A novel mechanism for the transcriptional regulation of Wnt
412   signaling in development. Genes Dev. 2011;25(17):1783-95.

413   29.   Tseng AS, Engel FB, Keating MT. The GSK-3 inhibitor BIO promotes proliferation in
414   mammalian cardiomyocytes. Chemistry & biology. 2006;13(9):957-63.

415   30.   Sato N, Meijer L, Skaltsounis L, Greengard P, Brivanlou AH. Maintenance of pluripotency in
416   human and mouse embryonic stem cells through activation of Wnt signaling by a
417   pharmacological GSK-3-specific inhibitor. Nature medicine. 2004;10(1):55-63.

418   31.   Meijer L, Skaltsounis AL, Magiatis P, Polychronopoulos P, Knockaert M, Leost M, et al.
419   GSK-3-selective inhibitors derived from Tyrian purple indirubins. Chemistry & biology.
420   2003;10(12):1255-66.

421   32.   Cohen P, Goedert M. GSK3 inhibitors: development and therapeutic potential. Nat Rev
422   Drug Discov. 2004;3(6):479-87.

423   33.   Patel P, Woodgett JR. Glycogen Synthase Kinase 3: A Kinase for All Pathways? Curr Top
424   Dev Biol. 2017;123:277-302.

425   34.   Hur EM, Zhou FQ. GSK3 signalling in neural development. Nat Rev Neurosci.
426   2010;11(8):539-51.

427   35.   Blackledge NP, Zhou JC, Tolstorukov MY, Farcas AM, Park PJ, Klose RJ. CpG islands
428   recruit a histone H3 lysine 36 demethylase. Mol Cell. 2010;38(2):179-90.

429   36.   He TC, Sparks AB, Rago C, Hermeking H, Zawel L, da Costa LT, et al. Identification of c-
430   MYC as a target of the APC pathway. Science. 1998;281(5382):1509-12.

431   37.   Lustig B, Jerchow B, Sachs M, Weiler S, Pietsch T, Karsten U, et al. Negative feedback
432   loop of Wnt signaling through upregulation of conductin/axin2 in colorectal and liver tumors.
433   Mol Cell Biol. 2002;22(4):1184-93.

434   38.   Jho EH, Zhang T, Domon C, Joo CK, Freund JN, Costantini F. Wnt/beta-catenin/Tcf
435   signaling induces the transcription of Axin2, a negative regulator of the signaling pathway.
436   Mol Cell Biol. 2002;22(4):1172-83.

437   39.   Tetsu O, McCormick F. Beta-catenin regulates expression of cyclin D1 in colon carcinoma
438   cells. Nature. 1999;398(6726):422-6.

17

439   40.   Shtutman M, Zhurinsky J, Simcha I, Albanese C, D'Amico M, Pestell R, et al. The cyclin D1
440   gene is a target of the beta-catenin/LEF-1 pathway. Proc Natl Acad Sci U S A.
441   1999;96(10):5522-7.

442   41.   Zhou Z, Yang X, He J, Liu J, Wu F, Yu S, et al. Kdm2b Regulates Somatic Reprogramming
443   through Variant PRC1 Complex-Dependent Function. Cell reports. 2017;21(8):2160-70.

444   42.   He J, Shen L, Wan M, Taranova O, Wu H, Zhang Y. Kdm2b maintains murine embryonic
445   stem cell status by recruiting PRC1 complex to CpG islands of developmental genes. Nat
446   Cell Biol. 2013;15(4):373-84.

447   43.   Kent WJ, Sugnet CW, Furey TS, Roskin KM, Pringle TH, Zahler AM, et al. The human
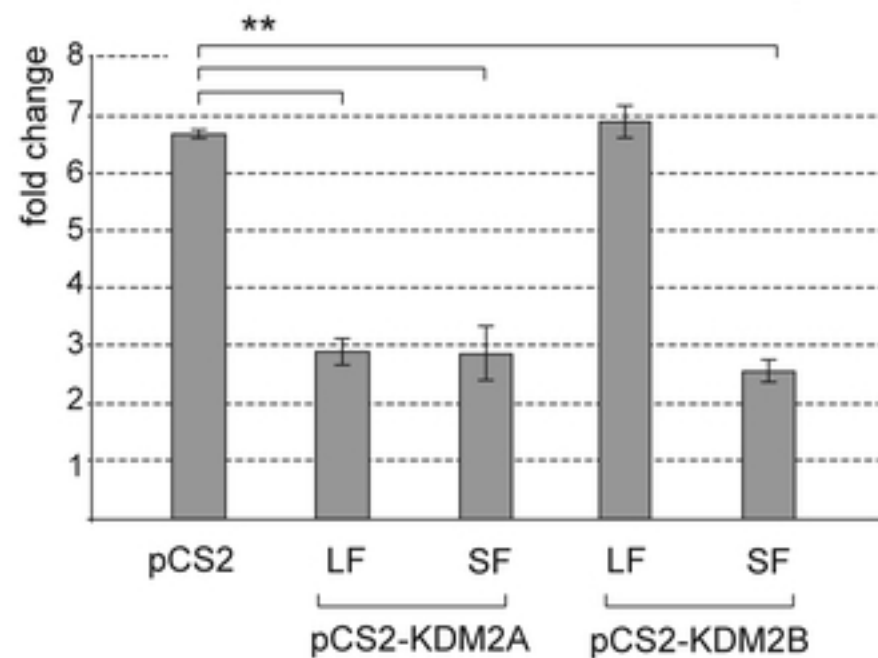448   genome browser at UCSC. Genome Res. 2002;12(6):996-1006.
449
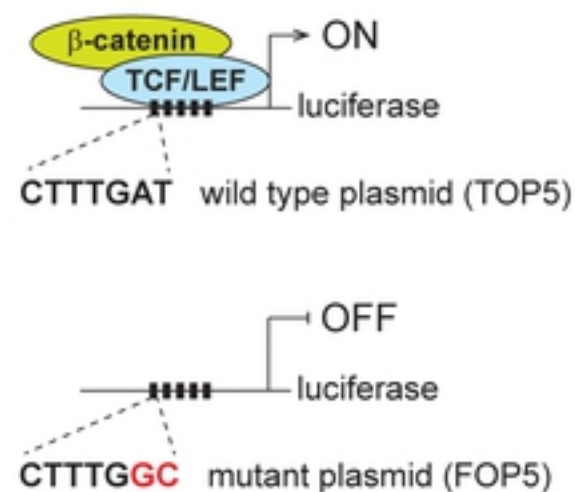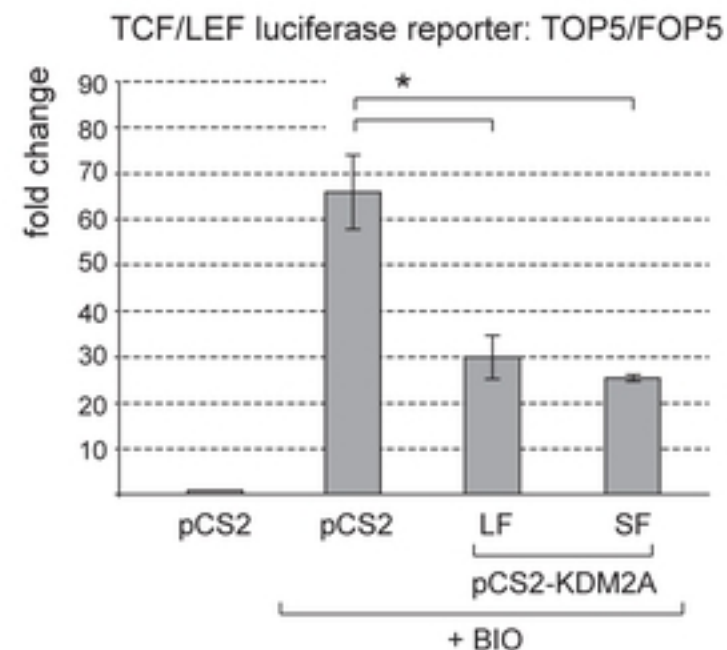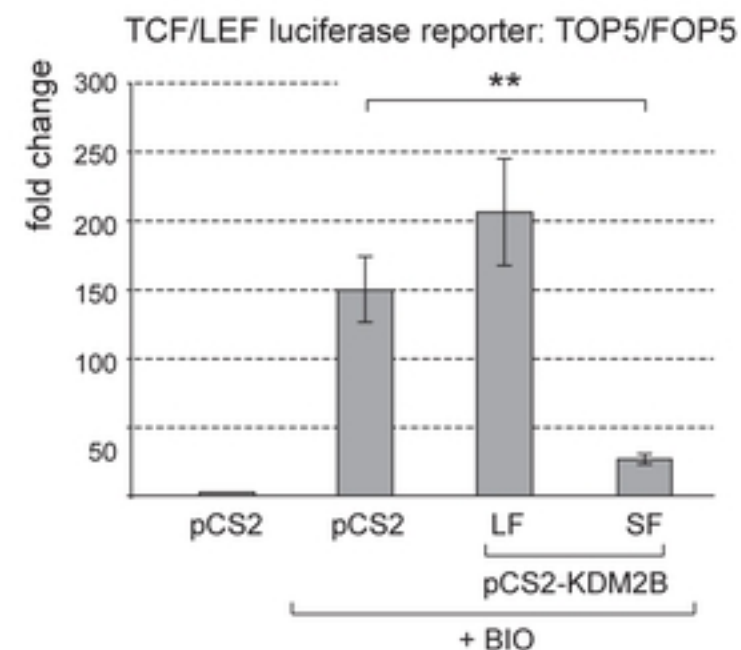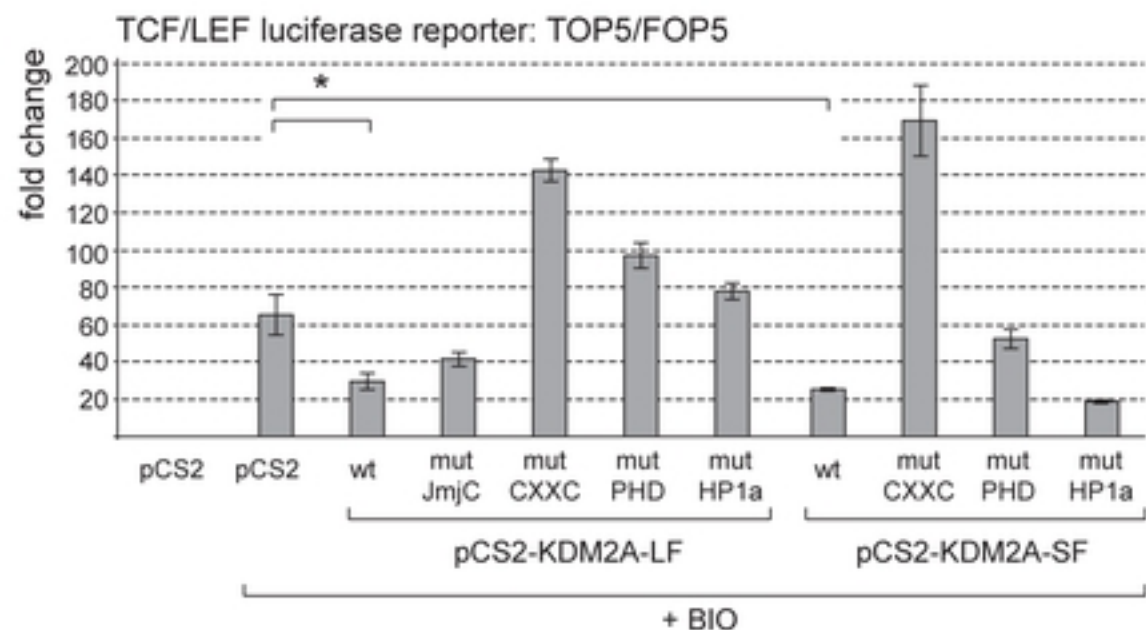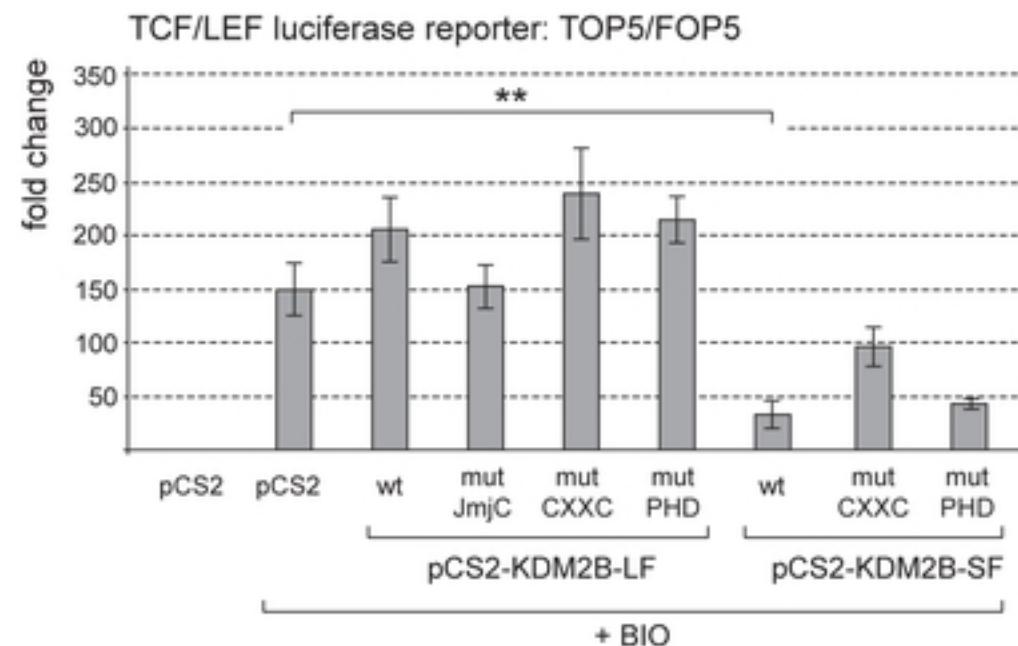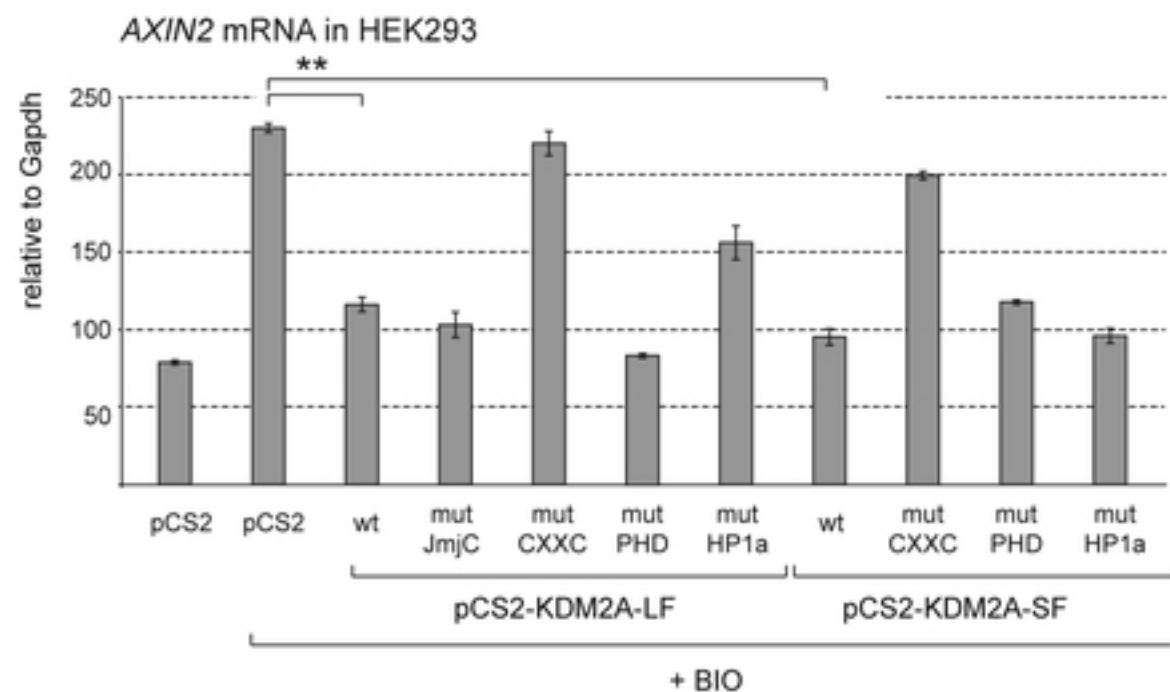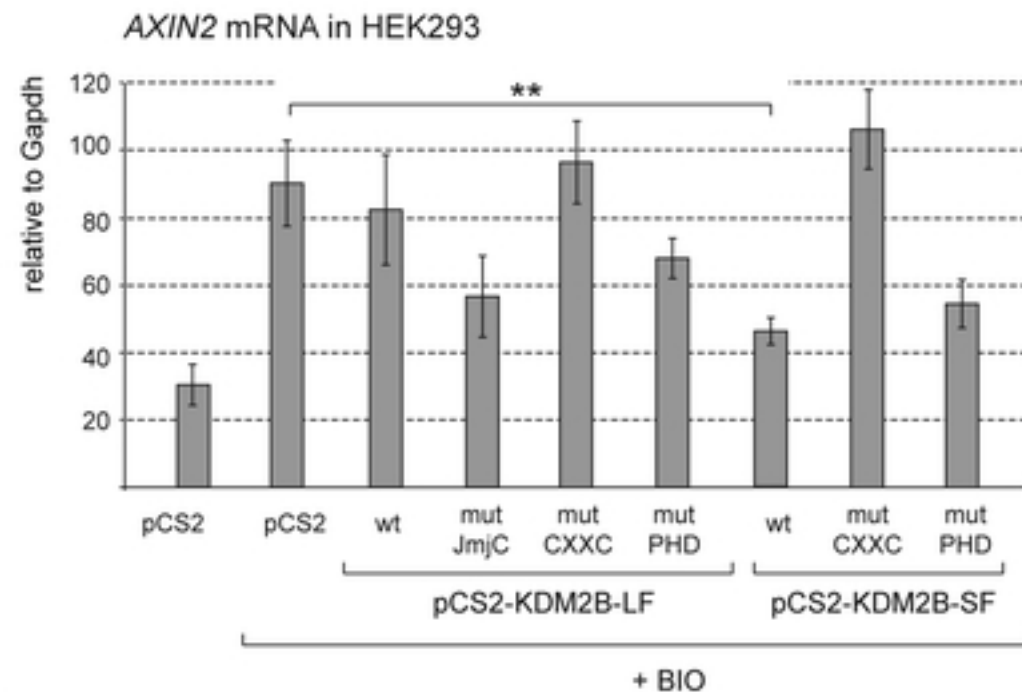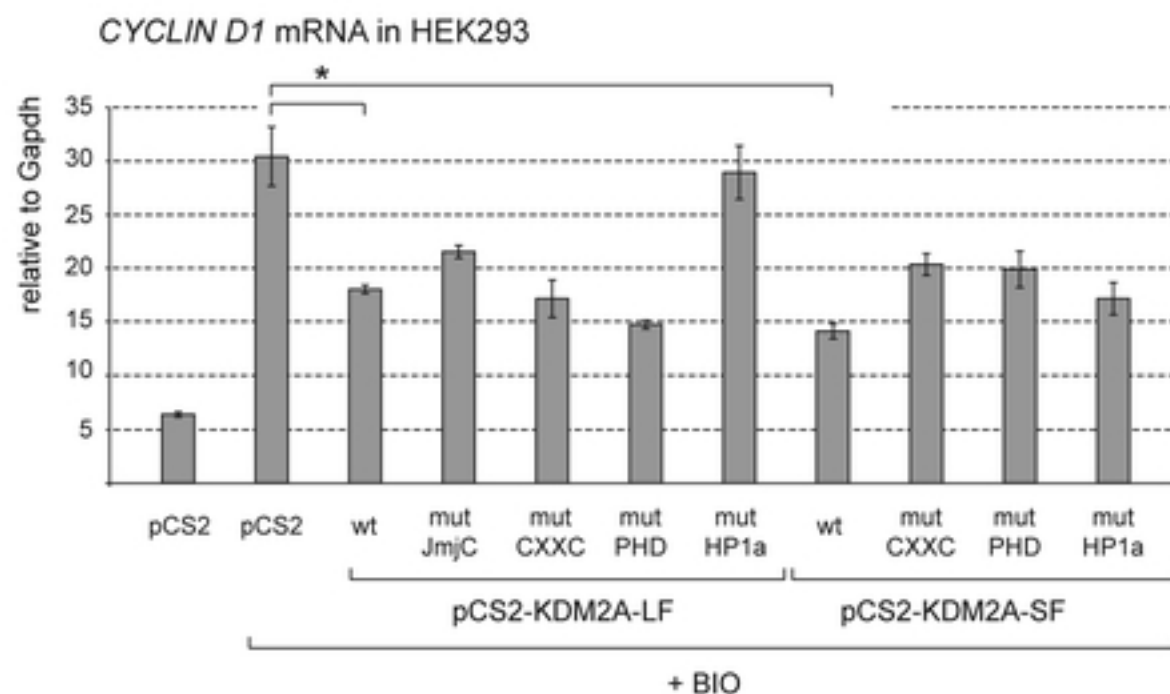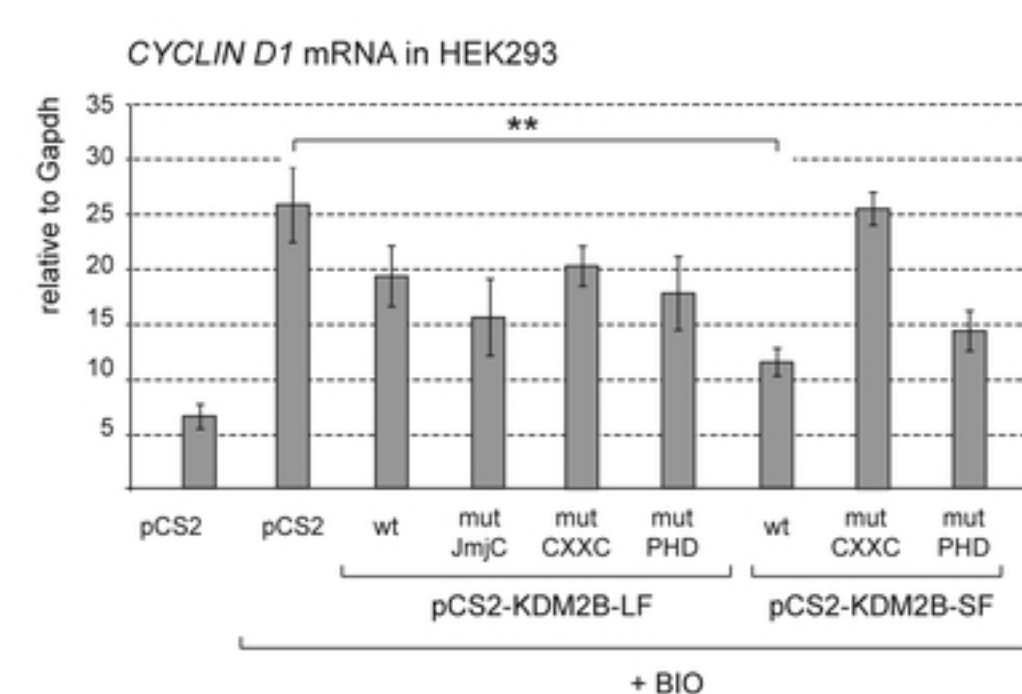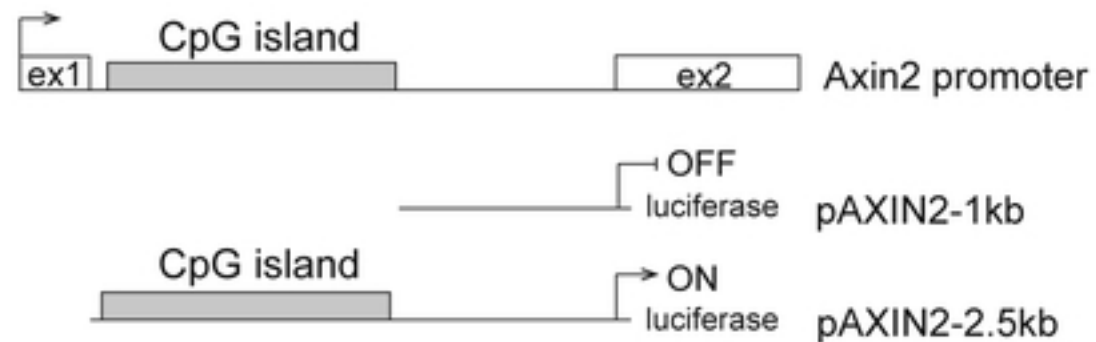
Figure 1

Figure 2

Figure 3

Figure 4

Figure 5